	<b>NewAthena</b> WFI simulator configuration	Ref. : WFI-ECAP-TNO-10-002_i1.19_SIXTE_Instrument_Configuration Date : 19 Sep 2025 Page : 1 of 13
--	--	---

## Abstract

For the *NewAthena* Wide Field Imager (WFI), the SIXTE package is provided with up-to-date configuration files to study the performance of the instrument. This document describes all relevant files included in the current release (version 1.11.3).

## Change Record

<i>Issue</i>	<i>Date</i>	<i>Description of Change</i>	<i>Affected Pages</i>
1	2014 October 02	Initial Release	All
2	2015 April 02	Update to new configuration	All
3	2017 August 17	Update to the QE table, include Be filter	All
4	2019 June 25	Update to new configuration	All
5	2019 Nov 12	Add background file description	11
6	2020 Nov 17	Update for prelim. release of resources for Red Book preparation (incl. telescope reference v3.1, updates to instrument description)	all
7	2020 Dec 09	Update mirror effective area (4 nm SiC overcoating)	9, 10
8	2021 Jan 28	Update PSF (bug fix in non-defocused version)	11
9	2021 Feb 25	Add PSF and XMLs for extremely degr. HEW (7")	7, 11
10	2021 April 20	Update PSF files version	11
11	2021 May 18	Add 6" and 8" on-axis HEW PSFs	7, 11
12	2021 May 27	Update defocused PSF	11, 12
13	2021 Oct 29	Add 9" and 10" on-axis HEW PSFs	7, 12
13	2021 Nov 19	Update QEs and ARFs	9, 10
14	2023 Jun 15	Update all to NewAthena	All
15	2024 Mar 08	Update ARFs, PSFs and Vignetting	All
16	2024 Oct 31	Update for SIXTE 3 and add second settling	6 – 8
17	2025 Jan 29	Update mirror effective area	9,10,11
18	2025 Feb 07	Add FD without OBF configuration	7, 9 – 11
19	2025 September 19	Update mirror effective area	9 – 11

## Distribution List

<i>Organization</i>	<i>Name</i>	<i>Organization</i>	<i>Name</i>	<i>Organization</i>	<i>Name</i>
MPE	K. Nandra	MPE	A. Rau	ECAP	J. Wilms

## Approvals

<i>Function</i>	<i>Name</i>	<i>Date</i>	<i>Signature</i>
Author	T. Dauser	19 Sep 2025	N/A
Author	M. Lorenz	19 Sep 2025	N/A
Author	L. Dauner	19 Sep 2025	N/A
Author	O. König	19 Sep 2025	N/A
Author	C. Kirsch	19 Sep 2025	N/A
Author	J. Wilms	19 Sep 2025	N/A



## Contents

<b>List of Figures</b>	<b>3</b>
<b>List of TBD Issues</b>	<b>3</b>
<b>List of TBC Issues</b>	<b>3</b>
<b>1 Introduction</b>	<b>6</b>
<b>2 Chip layouts and readout modes</b>	<b>6</b>
2.1 Chip geometry . . . . .	6
2.2 Chip Readout . . . . .	7
2.3 DEPFET readout implementation . . . . .	7
2.4 Pattern analysis in the DEPFET-case . . . . .	8
2.5 Simulated DEPFET chip layouts and readout modes . . . . .	8
<b>3 Calibration data</b>	<b>9</b>
<b>4 ARF</b>	<b>9</b>
4.1 Mirror Effective Area . . . . .	9
4.2 Quantum Efficiency . . . . .	9
4.3 ARF Construction . . . . .	10
4.4 RMF . . . . .	10
4.5 Vignetting . . . . .	11
4.6 PSF . . . . .	11
4.7 PHA background . . . . .	12
4.8 Charge cloud size . . . . .	12
<b>5 Conclusions</b>	<b>13</b>

**List of Figures**

1	Geometry of the <code>ld_wfi_ff_all_chips.xml</code> configuration of the LDA. . . . .	6
2	A basic scheme for the DEPFET readout. . . . .	7
3	Mirror effective area and final ARF configurations . . . . .	11
4	Width of the RMF in the relevant energy range. . . . .	11
5	Vignetting as a function of the off-axis angle for different photon energies. . . . .	12
6	The PSF at different energies and off-axis angles. . . . .	12

**List of TBD Issues**

**List of TBC Issues**

**List of Acronyms**



**ARF** : Ancillary Response File  
**NewAthena**: Advanced Telescope for High ENergy Astrophysics  
**DEPFET**: Depleted p-channel Field-Effect  
**OBF** : Optical Blocking Filter  
**PSF** : Point Spread Function  
**QE** : Quantum Efficiency  
**RMF** : Redistribution Matrix File  
**WFI** : Wide Field Imager  
**LDA** : Large Detector Array  
**FD** : Fast Detector

---



## Documentation

### Reference Documents

<i>Ref.</i>	<i>Title</i>	<i>Ref. Doc.-No.</i>
RD1	Athena WFI Response Files	WFI-ECAP-TNO-10_011_i1.15_Response_Files
RD2	WFI Defocus Study	ECAP-WFI-DFOPT-20160711
RD3	Instrument Efficiency (Rau, A.)	WFI-MPE-ANA-10-011
RD4	NewAthena mirror performance (E. Kuulkers, I. Ferreira, M. Guainazzi), Issue Nr. 1, Revision Nr. 2, 24/05/2023	i3 - 22.02.2023

### Reference Articles

---

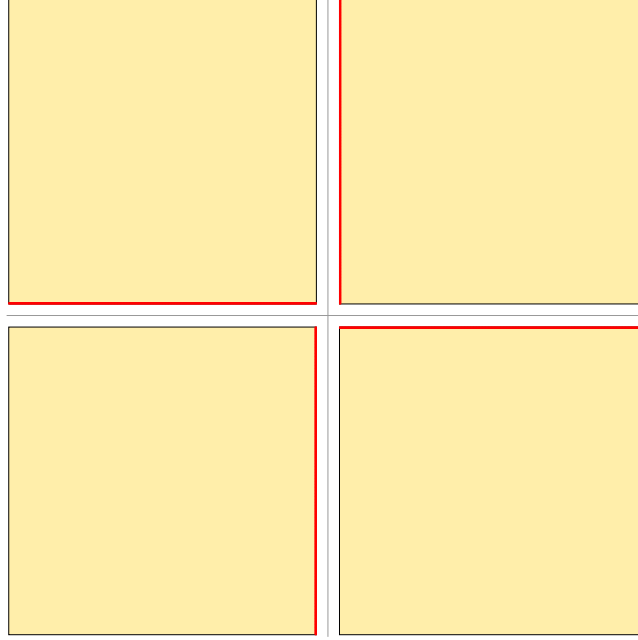


Figure 1: Geometry of the `1d_wfi_ff_all_chips.xml` configuration of the LDA. The gray cross marks the default intersection point with the optical axis. The gap width chosen for this configuration file is 5 mm.

## 1 Introduction

The SIXTE simulator is capable to simulate X-ray observations with pixelized detectors like the WFI. To achieve a high flexibility, the telescope and detector properties are fed into the program via a descriptive file in an XML-like format, which gives optical and detection parameters as well as links to files containing calibration information. These information are contained in FITS-files encoding for example the PSF, the vignetting curve, the ARF or the RMF. This document lists all available configurations and calibration files for the current iteration of the *NewAthena* WFI.

## 2 Chip layouts and readout modes

The available WFI setups for SIXTE simulations are listed in Table 1. There are options for the full Large Detector Array (LDA) of the WFI with 4 large chips, called the Large Detectors (LD). Moreover, readout modes for the separate Fast Detector (FD) are given, which will be mounted defocused by default. All WFI chips will employ the Depleted p-channel Field-Effect (DEPFET) technology, which is described below and requires a different implementation of the readout than the CCDs used for previous missions like *XMM-Newton* or *SRG/eROSITA*. In the following the single modi and their implementation is described in more detail.

### 2.1 Chip geometry

The individual chips are realized as rectangular surfaces with a rectangular, uniform subdivision. The resulting rectangles are the equivalent of the pixels. The number of pixels and their sizes are listed in Table 1. The first entry in this table corresponds to the four large chips with their individual alignment and rotation (LDA). The gap between the chips is 5 mm, and the optical axis is located at the center of the assembly. The geometrical configuration of this case can be seen in Fig. 1.

Table 1: Chip and read-out data of the simulated DEPFET setups. The read-out time per line is set to  $3.9\ \mu\text{s}$  for the LDs and  $2.5\ \mu\text{s}$  for the FD. The LD modes are given for a PSF with a nominal on-axis HEW of  $9''$ . The FD is assumed to be defocused by default. Most configurations are given without (wo) and with (w) Optical Blocking Filter (OBF), provided in separate directories (`wfi_wo_filter` and `wfi_w_filter`). For the FD, there is also a configuration with a thick filter.

Name	Filename	Size (rows $\times$ columns)	time resolution	defocusing	filter
<i>full</i>	<code>ld_wfi_ff_all_chips.xml</code>	$(4 \times) 512 \times 512$	$1997\ \mu\text{s}$	—	wo/w
<i>single</i>	<code>ld_wfi_ff_chip[0,1,2,3].xml</code>	$512 \times 512$	$1997\ \mu\text{s}$	—	wo/w
<i>large</i>	<code>ld_wfi_ff_large.xml</code>	$512 \times 512$	$1997\ \mu\text{s}$	—	wo/w
<i>w128</i>	<code>ld_wfi_w128.xml</code>	$128 \times 512$	$499\ \mu\text{s}$	—	wo/w
<i>w256</i>	<code>ld_wfi_w256.xml</code>	$256 \times 512$	$998\ \mu\text{s}$	—	wo/w
<i>fast</i>	<code>fd_wfi_df35mm.xml</code>	$64 \times 64$	$80\ \mu\text{s}$	35 mm	wo/w
<i>fastThickFilter</i>	<code>fd_wfi_df35mm_thick_filter.xml</code>	$64 \times 64$	$80\ \mu\text{s}$	35 mm	w

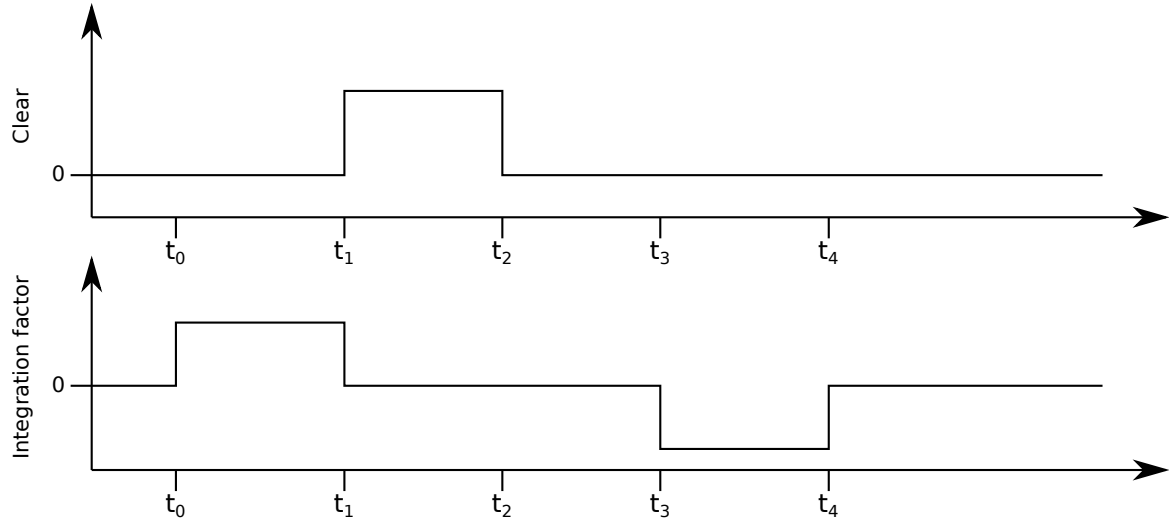


Figure 2: A basic scheme for the DEPFET readout.

## 2.2 Chip Readout

Setups for the LDA (*full*), the single LDs (*single*), a single LD with the aim point in the center (*large*), and window modes (*w128* and *w256*), where only part of the chip is read out in order to mitigate pile-up, are available.

Each half of the Fast Detector (FD) is read out separately, additionally increasing the readout speed by a factor of two. It will be mounted 35 mm out of focus. An out-of-focus distance of around 35 mm was determined to be most favourable. More details on this study can be found in [RD2].

## 2.3 DEPFET readout implementation

The following section describes the implementation of the WFI DEPFET. The DEPFET readout is not an instantaneous determination of the photon's energy but it integrates first the photon's voltage signal together with the signal baseline, and after the photon's charge is removed by the clear, the baseline is integrated again to remove it from the measurement. In a simplified scheme, the measurement can be described with three time intervals and the corresponding integration factors, as depicted in Fig. 2.

After the initial settling, the readout of a DEPFET begins at  $t_0$ . Between  $t_0$  and  $t_1$ , the signal present at the

Table 2: The DEPFET time characteristics used in the simulations for the LD and FD.

	integration time [ $\mu s$ ]	first settling time [ $\mu s$ ]	second settling time [ $\mu s$ ]	clear time [ $\mu s$ ]
Large Detector	1.0	0.5	0.4	1.0
Fast Dectector	0.8	0.3	0.3	0.3

internal gate is integrated. Between  $t_1$  and  $t_2$ , any charge is removed from the DEPFET's internal gate. Between  $t_2$  and  $t_3$ , the second settling occurs. Between  $t_3$  and  $t_4$ , the signal is integrated again but with negative sign. The result is, that the baseline signal can be subtracted from the first measurement, providing an estimate of the photon's signal.

Misfits are photons which hit the detector during the integration time intervals. As their signal is not integrated for the full integration time, they can produce wrong measurements. The resulting measurement  $E_m$  of their true energy  $E_p$  can be described dependent on their impact time  $t_p$ :

- $t_p < t_0$  or  $t_p > t_4$ :  $E_m = E_p$
- $t_0 < t_p < t_1$ :  $E_m = E_p \times (t_1 - t_p)/(t_1 - t_0)$
- $t_2 < t_p < t_3$ :  $E_m = -E_p$
- $t_3 < t_p < t_4$ :  $E_m = -E_p \times (t_4 - t_p)/(t_4 - t_3)$

In the case of  $t_3 < t_p < t_4$ , the charge is not removed in this readout cycle and will be measured again during the next cycle, before it is cleared.

Another effect to be simulated is the limited clear speed. Instead of removing the charge instantaneously, it is cleared linearly between  $t_1$  and  $t_2$ . If a photon hits the detector during this interval and causes a charge  $q_p$ , it is only partially cleared and leaves a remaining charge  $q_r$ , according to

$$q_r = q_p \times (t_p - t_1)/(t_2 - t_1) .$$

The remaining charge will be measured in the second integration time and causes a negative energy measurement of the value

$$E_m = -E_p \times (t_p - t_1)/(t_2 - t_1) .$$

The charge will be measured again in the next readout cycle.

If the impact is between  $t_2$  and  $t_3$ , the charge is remaining completely. If two photons impact in the same pixel during one readout cycle, their signals add to each other.


## 2.4 Pattern analysis in the DEPFET-case

The normal pattern analysis is used also for DEPFET-data. Patterns which include at least one split partner with a negative energy measurement are flagged as invalid. Patterns are not traced over more than one frame.

## 2.5 Simulated DEPFET chip layouts and readout modes

In Table 1, the implemented setups are listed. The DEPFET time characteristics are listed in Table 2.



	<i>NewAthena</i> WFI simulator configuration	Ref. : WFI-ECAP-TNO-10-002_i1.19_SIXTE_Instrument_Configuration Date : 19 Sep 2025 Page : 9 of 13
---	--	---

### 3 Calibration data

For simulations of astronomical observations with the *NewAthena* WFI, calibration files such as the ARF, RMF, or their product, the RSP, are needed. In this section, we describe the current set of ARFs and RMFs. The general WFI response files are described in the separate document [RD1].

## 4 ARF

The WFI ARF is composed of two inputs: The mirror effective area and the instrument efficiency (incl. sensor and OBF).

### 4.1 Mirror Effective Area

The mirror effective area is based on the mirror geometry as described in [RD4], with parameters reflecting the latest adjustments:

- Mirror assembly with 13 rows
- Membrane thickness 0.11 mm
- Mirror plate rib spacing (pitch) of 2.38 mm
- Rib thickness of 0.17 mm
- Tri-layer coating (Cr[12.5/0.45],Pt[10/0.45],C[8/0.45], where thickness/roughness in nm)
- -1/+1 wedging geometry

The data file containing the mirror effective area is called AeffPtins-8Sep.txt, from 15 September 2025, provided by A. Rau.

### 4.2 Quantum Efficiency

The sensor Quantum Efficiency (QE) and filter transmission values were provided by M. Barbera and compiled in [RD3]. The final instrument efficiency depends on the configuration used. The single contributions are:

**Sensor QE:** 450  $\mu$ m Si detector absorbing layer

**On-Chip OBF:** 20 nm SiO<sub>2</sub> + 30 nm Si<sub>3</sub>N<sub>4</sub> + (86.5+8.65) nm Al + 3.5 nm Al<sub>2</sub>O<sub>3</sub> (incl. 10% margin on Al)


**Filter wheel OBF:** 150nm Polyimide + (23+5) nm Al + 7 nm Al<sub>2</sub>O<sub>3</sub> (incl. 5 nm margin on Al)

**Honeycomb mesh:**

LDA: 4.8 mm pitch, 150  $\mu$ m SS + 10  $\mu$ m Au wire thickness, 75  $\mu$ m SS + 10  $\mu$ m Au wire width

FD: 4.8 mm pitch, 80  $\mu$ m SS + 10  $\mu$ m Au wire thickness, 40  $\mu$ m SS + 10  $\mu$ m Au wire width

**Thick Filter:** Polyimide 25  $\mu$ m + Al 43+5 nm + Al 43+5 nm + Al<sub>2</sub>O<sub>3</sub> 14 nm, incl. 5 nm margin on both Al (available for Fast Detector only)

	<b>NewAthena</b> WFI simulator configuration	Ref. : WFI-ECAP-TNO-10-002_i1.19_SIXTE_Instrument_Configuration Date : 19 Sep 2025 Page : 10 of 13
---	--	--

The data also includes estimates of the in-orbit molecular contamination (**Cont\_DBP**), particle contamination (**Cont\_PAC**), an average blocking factor of the **LDA OBF stiffening cross** of 2.3%, and an overall system level **margin** of 2%. From this information we can define the four cases of interest for the WFI.

- **Case 1** (LDA w/o OBF): Sensor QE, on-chip OBF, Cont\_DBP, Cont\_PAC, and margin  
(WFI-eff\_LDA\_wo\_filter\_sixte\_20220308.dat)
- **Case 2** (LDA w/ OBF): Sensor QE, on-chip OBF, filter wheel OBF, LDA honeycomb mesh, LDA OBF stiffening cross, Cont\_DBP, Cont\_PAC, and margin  
(WFI-eff\_LDA\_w\_filter\_sixte\_20220308.dat)
- **Case 3** (FD w/o OBF): Sensor QE, on-chip OBF, Cont\_DBP, Cont\_PAC, and margin  
(WFI-eff\_FD\_wo\_filter\_sixte\_20220308.dat)
- **Case 4** (FD w/ OBF): Sensor QE, on-chip OBF, filter wheel OBF, FD honeycomb mesh, Cont\_DBP, Cont\_PAC, and margin  
(WFI-eff\_FD\_w\_filter\_sixte\_20220308.dat)
- **Case 5** (FD w/ thick filter): Sensor QE, on-chip OBF, thick filter, Cont\_DBP, Cont\_PAC, and margin  
(WFI-eff\_FD\_w\_thick\_filter\_sixte\_20220308.dat).

### 4.3 ARF Construction

The ARF is the result of the multiplication of the mirror effective area and the quantum efficiency. Taking the above cases of the quantum efficiency effects and the mirror area into account, the following ARFs are provided:

1. athena\_wfi\_sixte\_13rows\_wo\_filter\_LDA\_v20250919.arf (LDA w/o OBF)
2. athena\_wfi\_sixte\_13rows\_w\_filter\_LDA\_v20250919.arf (LDA w/ OBF)
3. athena\_wfi\_sixte\_13rows\_wo\_filter\_FD\_v20250919.arf (FD w/o OBF)
4. athena\_wfi\_sixte\_13rows\_w\_filter\_FD\_v20250919.arf (FD w/ OBF)
5. athena\_wfi\_sixte\_13rows\_w\_thick\_filter\_FD\_v20250919.arf (FD w/ thick filter)

The mirror effective area and ARFs for all cases are shown in Fig. 3.

### 4.4 RMF

The RMF has been constructed in an energy range from 0.02 keV to 15 keV with a step size of 0.01 keV in both Energy and EBOUNDS.

The RMF is composed of a Gaussian curve integrated in the respective EBOUNDS-bins, with a width that was fit to FD lab measurements (parameters provided by A. Rau, representing the expected EOL performance).

The width is described by the formula

$$\sigma(E) = (A * E + B)/2.355, \quad (1)$$

where  $E$  is the energy in electronvolts,  $A = 0.0103$  and  $B = 87.67$ .

The resolution is shown in Fig. 4. The RMF is available as athena\_wfi\_sixte\_v20230523.rmf .

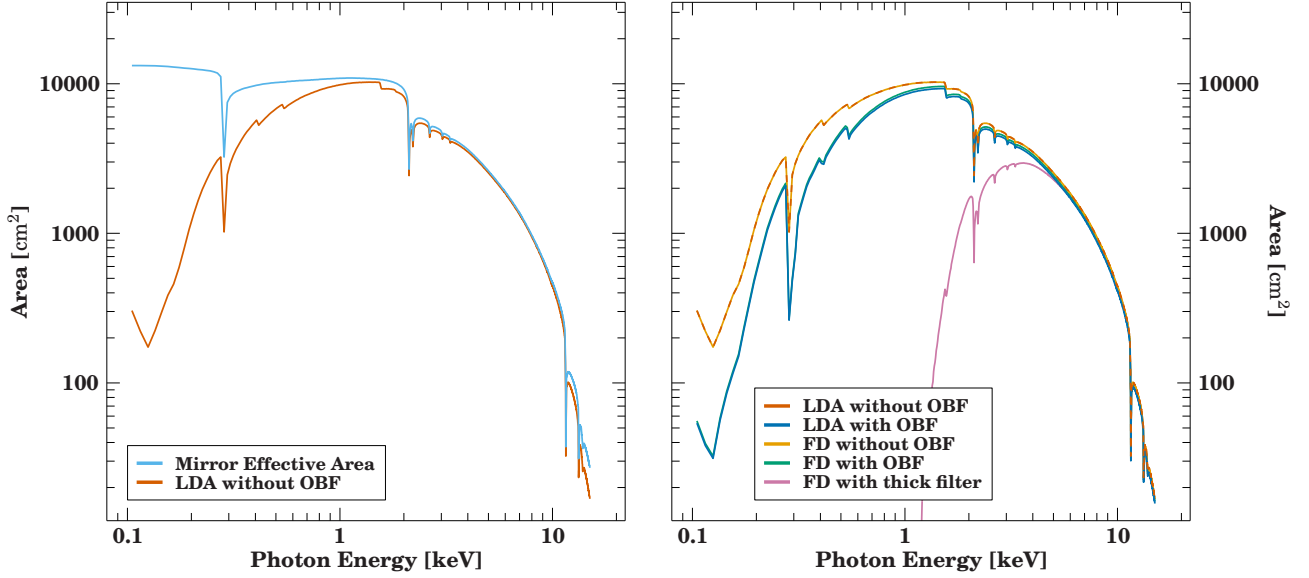


Figure 3: The mirror effective area and the final ARF configuration for the LDA without OBF are shown on the left. The right panel shows the resulting ARFs for all cases of interest. The assumptions entering the effective area are described in the text.

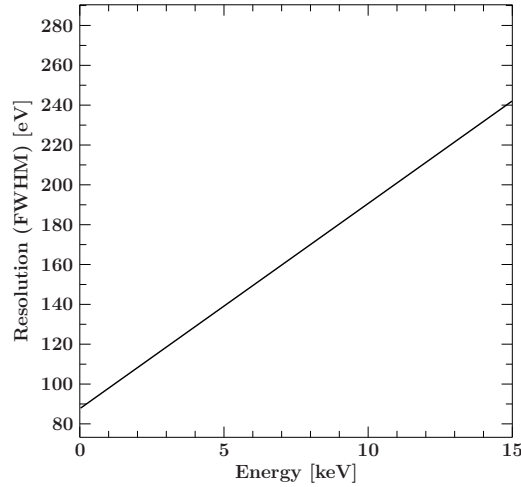


Figure 4: The width of the RMF in the relevant energy range.

## 4.5 Vignetting

The vignetting is described in the file `athena_vig_13rows_20231211.fits` (based on [RD4]) and can be seen in Fig. 5.

## 4.6 PSF

For the PSF we use the file `athena_psf_hew9_20231211.fits` for the nominal on-axis HEW requirement (9"). A modified pseudo-Voigt distribution is used for the PSF model with parameters provided in [RD4]. The defocused PSF is taken from ray-tracing simulations (R. Willingale), using the file `athena_psf_defoc_20231211.fits`.

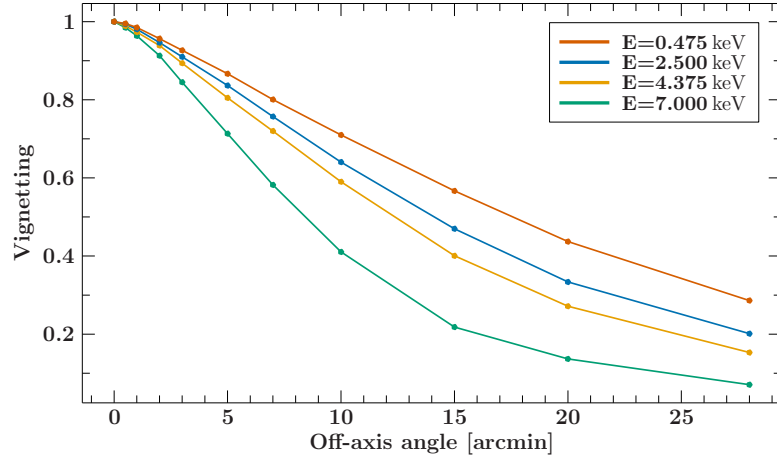


Figure 5: The vignetting as a function of the off-axis angle for different photon energies.

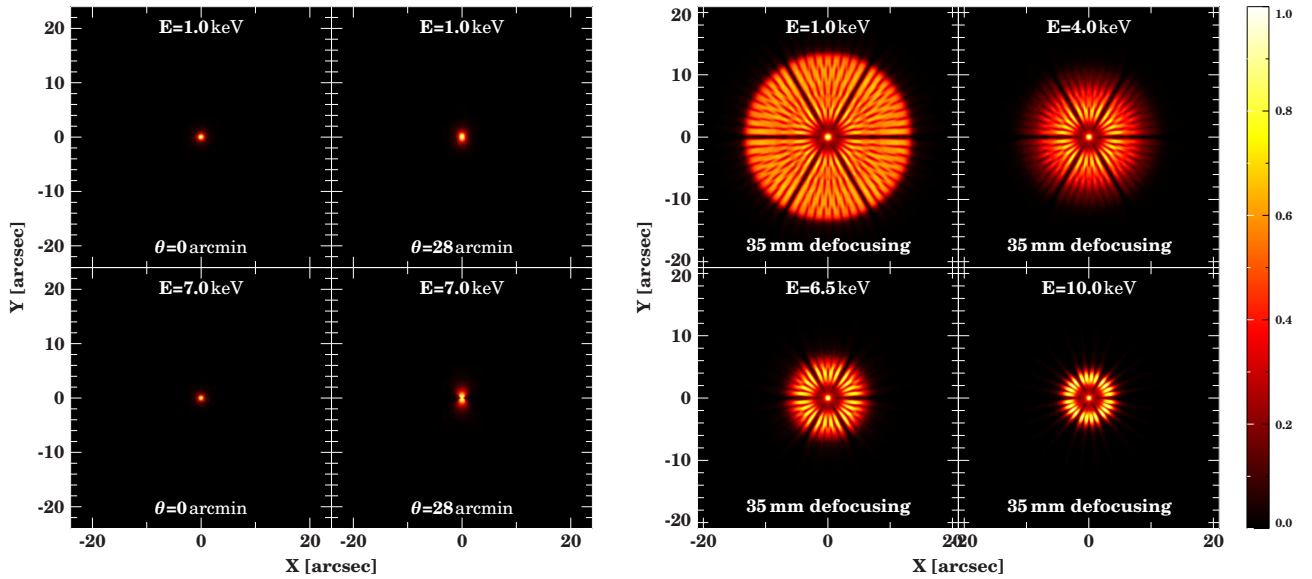


Figure 6: The PSF at different energies and off-axis angles. The left panel shows the PSF corresponding to an angular resolution of 9" HEW on-axis, while the right panel shows the defocused PSF for the FD for 35 mm defocusing at different energies. Note that the effect of defocusing is strongly energy dependent.

The PSFs are shown in Fig. 6 for different energies and off-axis angles.

#### 4.7 PHA background

The instrumental background is specified in the file `sixte_wfi_particle_bkg_20230602_nxb8.pha`. It corresponds to a flat spectrum of  $8 \cdot 10^{-3} \text{ cts s}^{-1} \text{ cm}^{-2} \text{ keV}^{-1}$  across the whole instrument ARF.

#### 4.8 Charge cloud size

The charge cloud size is fixed to  $11 \mu\text{m}$ .



## 5 Conclusions

The setups described in this document can be used to run up-to-date simulations for the *NewAthena* WFI with the SIXTE package. The version described in this document is v1.11.3.

These files should only be used with SIXTE. Questions regarding the setup and the simulations should be directed to [sixte-support@lists.fau.de](mailto:sixte-support@lists.fau.de).